



OPEN

## Preclinical immunological characterization of rademikibart (CBP-201), a next-generation human monoclonal antibody targeting IL-4R $\alpha$ , for the treatment of Th2 inflammatory diseases

Limin Zhang<sup>1</sup>, Ying Ding<sup>1</sup>, Qingjian Wang<sup>2</sup>, Wubin Pan<sup>1</sup>, Zheng Wei<sup>2</sup>, Paul A. Smith<sup>2</sup> & Xin Yang<sup>1</sup>✉

Rademikibart (CBP-201) is a next-generation human monoclonal antibody targeting IL-4R $\alpha$ , undergoing evaluation in Phase 2 clinical trials for the treatment of moderate-to-severe Th2 inflammatory diseases. We report the immunological characterization of rademikibart. Rademikibart and dupilumab were associated with  $K_D$  of 20.7 pM and 45.8 pM, respectively, when binding to distinct human IL-4R $\alpha$  epitopes. Rademikibart did not bind to IL-4R $\alpha$  from other species. Rademikibart inhibited IL-4 and IL-13-mediated STAT6 signaling (mean  $\pm$  SD  $IC_{50}$ : 7.0  $\pm$  2.5 and 6.6  $\pm$  1.5 ng/mL, respectively), TF-1 cell proliferation ( $IC_{50}$ : 8.0  $\pm$  1.6 and 9.7  $\pm$  0.8 ng/mL, respectively) and TARC production in PBMCs ( $IC_{50}$ : 59.2  $\pm$  3.9 and 13.5  $\pm$  0.2 ng/mL, respectively). Rademikibart versus dupilumab was more potent in the STAT6 assays (IL-4,  $p < 0.01$ ; IL-13,  $p = 0.03$ ), with non-significant trends towards greater potency in the TF-1 cell assays (IL-4,  $p = 0.09$ ; IL-13,  $p = 0.20$ ), and similar potency in the TARC assays. In experiments with mice expressing human IL-4R $\alpha$  and IL-4, rademikibart and dupilumab demonstrated similar potency; both monoclonal antibodies eliminated IL-4 ( $p < 0.0001$ ) and IL-13 ( $p < 0.05$ ) mediated B cell activation in vitro and ovalbumin-induced IgE ( $p < 0.01$ ) and eosinophilic lung infiltration ( $p < 0.0001$ ) in vivo. In Th2-stimulated human skin explants, rademikibart rapidly downregulated IL-4, IL-13, and TARC gene expression, with greater effectiveness than dupilumab for IL-4 ( $p < 0.01$ ) and a non-significant trend towards superiority for IL-13. In summary, rademikibart bound to a distinct IL-4R $\alpha$  epitope with high affinity and demonstrated reductions in Th2 inflammatory biomarkers with at least similar and potentially superior potency to dupilumab.

T helper-2 (Th2) inflammatory diseases including asthma and atopic dermatitis (AD) affect a large proportion of the worldwide population, with prevalence varying by age, clinical definitions, country, and sampling methods<sup>1–14</sup>. Among adults and children in the US, prevalence estimates of 8.4% and 5.8% have been reported for asthma, and 7.2% and 12.5% for AD, respectively<sup>9–14</sup>. In adults, the estimated global prevalence of asthma symptoms (8.6%) is similar per continent (Latin America 7.6%, Europe 10.7%) with some variation by country (Australia 27.4%)<sup>1</sup>, while AD may be most prevalent in Sweden (11.5%)<sup>8</sup>.

Asthma and AD are often inadequately controlled<sup>15–17</sup>. In the US, millions of work/school days are lost each year due to asthma attacks, which can lead to hospital admission and even death<sup>12,15,18</sup>. AD is characterized by recurrent eczematous lesions and intense pruritus, resulting in disturbed sleep, embarrassment, and increased risk of anxiety, depression, and suicidal ideation<sup>10,11,19–22</sup>. Use of medications for AD may be limited by adverse events and inefficacy<sup>17,23</sup>.

<sup>1</sup>Suzhou Connect Biopharmaceuticals, Ltd, East R&D Building, 6 Beijing West Road, Taicang 214500, China. <sup>2</sup>Connect Biopharma LLC, 12265 El Camino Real, San Diego, CA 92130, USA. ✉email: xyang@connectpharm.com

Two proinflammatory Th2 cytokines, interleukin (IL)-4 and IL-13, and their cognate receptor (IL-4R $\alpha$ ), are key drivers of AD and asthma pathogenesis<sup>24–26</sup>. IL-4 and IL-13 are overexpressed in both diseases<sup>24,25,27–29</sup>. Other biomarkers of Th2 inflammatory diseases include thymus and activation-regulated chemokine (TARC), which recruits Th2 cells to inflammatory sites<sup>24,30,31</sup>, and over-secretion of IgE by B cells<sup>24,25</sup>. IL-4 and IL-13 promote IgE synthesis<sup>24,25</sup>. Monoclonal antibody therapies that selectively target IL-4R $\alpha$  or IL-13 have demonstrated favorable efficacy, pharmacodynamics, safety, and tolerability in clinical trials and real-world studies of Th2-driven inflammatory diseases, including AD and asthma<sup>24,32–40</sup>.

Rademikibart (CBP-201), a next-generation monoclonal antibody targeting IL-4R $\alpha$ , is undergoing evaluation in Phase 2 clinical trials in patients with moderate-to-severe Th2 inflammatory diseases, including AD (NCT04444752; NCT05017480) and persistent asthma (NCT04773678). Here, we report the first immunological characterization of rademikibart, assessed *in vitro* in a diverse collection of cellular systems, *in vivo* in a mouse model of Th2 inflammatory disease, and *ex vivo* in human skin.

## Results

**Rademikibart binds with high affinity to human IL-4R $\alpha$  via a distinct epitope.** Rademikibart and dupilumab were associated with  $K_D$  of 20.7 pM and 45.8 pM, respectively, for binding to human IL-4R $\alpha$  (Table 1). As shown by mutational analysis, rademikibart and dupilumab bound to distinct epitopes on human IL-4R $\alpha$  (Fig. 1 and Supplementary Fig. 1). Mutation of amino acid residues that are crucial for IL-4 binding had little effect on the affinity for dupilumab but abolished binding of rademikibart.

**Rademikibart is specific for human IL-4R $\alpha$ .** Cross-species ELISA revealed that rademikibart bound to human sIL-4R $\alpha$  with a  $K_D$  of 106 pM and  $IC_{50}$  of 4.9 ng/mL, but did not cross react with IL-4R $\alpha$  isolated from monkey, mouse, dog, rat, or rabbit (Fig. 2).

**Rademikibart inhibits cytokine-induced intracellular signaling.** In the human embryonic kidney (HEK) Blue™ reporter cell assay, incubation with rademikibart resulted in concentration-dependent inhibition of STAT6 intracellular signaling, which had been activated by IL-4 or IL-13 (Table 2 and Supplementary Fig. 2). When compared head-to-head, rademikibart was associated with significantly greater STAT6 inhibition than with dupilumab in cells stimulated with IL-4 (mean  $\pm$  standard deviation [SD]  $IC_{50}$ : 7.0  $\pm$  2.5 vs 9.9  $\pm$  2.7 ng/mL;  $p < 0.01$ ) and IL-13 (6.6  $\pm$  1.5 vs 9.7  $\pm$  2.5 ng/mL;  $p = 0.03$ ).

**Rademikibart binds strongly to TF-1 cells, inhibiting cytokine-induced TF-1 cell proliferation.** Rademikibart bound strongly to TF-1 cells (Supplementary Fig. 3). Moreover, rademikibart inhibited cytokine-induced TF-1 cell proliferation in a concentration-dependent manner, with non-significant trends towards greater potency than dupilumab following stimulation with IL-4 (mean  $\pm$  SD  $IC_{50}$ : 8.0  $\pm$  1.6 vs 10.8  $\pm$  1.1 ng/mL;  $p = 0.09$ ) and IL-13 (9.7  $\pm$  0.8 vs 12.0  $\pm$  2.4 ng/mL;  $p = 0.20$ ) (Table 2 and Supplementary Fig. 2).

**Rademikibart inhibits cytokine-induced TARC release.** Primary human peripheral blood mononuclear cells (PBMCs), when activated *in vitro* with either IL-4 or IL-13, released TARC into the culture supernatant. Rademikibart and dupilumab demonstrated similar potency when inhibiting TARC release stimulated by IL-4 (mean  $\pm$  SD  $IC_{50}$ : 59.1  $\pm$  1.2 vs 65.2  $\pm$  1.1 ng/mL;  $p = 0.11$ ) and IL-13 (13.6  $\pm$  1.1 vs 10.6  $\pm$  1.0 ng/mL;  $p = 0.41$ ) (Table 2 and Supplementary Fig. 2).

**Rademikibart inhibits cytokine-induced B cell activation.** IL-4 and IL-13 stimulation of splenocytes, isolated from commercially available genetically modified mice (double humanized IL-4/IL-4R $\alpha$  [B-hIL4/hIL4R $\alpha$ ]), resulted in 3.0-fold and 1.7-fold increases in CD23 and MHCII expression, respectively. Large, statistically significant decreases in the expression of both molecules were observed with all concentrations of rademikibart (0.1, 1.0, and 10.0  $\mu$ g/mL; 3 mice per group); CD23 ( $p < 0.0001$ ) and MHCII ( $p < 0.05$ ) returned to unstimulated levels with rademikibart 1.0  $\mu$ g/mL and 0.1  $\mu$ g/mL (Fig. 3). B cell responses to rademikibart were similar in magnitude to those with dupilumab.

Protocol	Immobilized protein	Analyte	1:1 binding		
			$k_a$ (1/Ms)	$k_d$ (1/s)	$K_D$ (pM)
A	sIL-4R $\alpha$	Rademikibart	$1.54 \times 10^7$	$3.19 \times 10^{-4}$	20.7
	sIL-4R $\alpha$	Dupilumab	$7.71 \times 10^6$	$3.53 \times 10^{-4}$	45.8
B	Rademikibart	sIL-4R $\alpha$	$6.51 \times 10^5$	$2.92 \times 10^{-4}$	448
	Dupilumab	sIL-4R $\alpha$	$6.41 \times 10^5$	$3.31 \times 10^{-4}$	516

**Table 1.** Rademikibart binds with high affinity to human IL-4R $\alpha$ . Two surface plasmon resonance protocols were used. *Protocol A*: Histidine tagged sIL-4R $\alpha$  was immobilized onto a treated CM5 sensor chip, to capture rademikibart or dupilumab analytes at different concentrations. *Protocol B*: Rademikibart or dupilumab were immobilized onto IgG Fc CM5 sensor chips, to capture sIL-4R $\alpha$  analyte at different concentrations.  $k_a$  association rate constant,  $k_d$  dissociation rate constant,  $K_D$  equilibrium dissociation constant, sIL-4R $\alpha$  soluble IL-4R $\alpha$ .

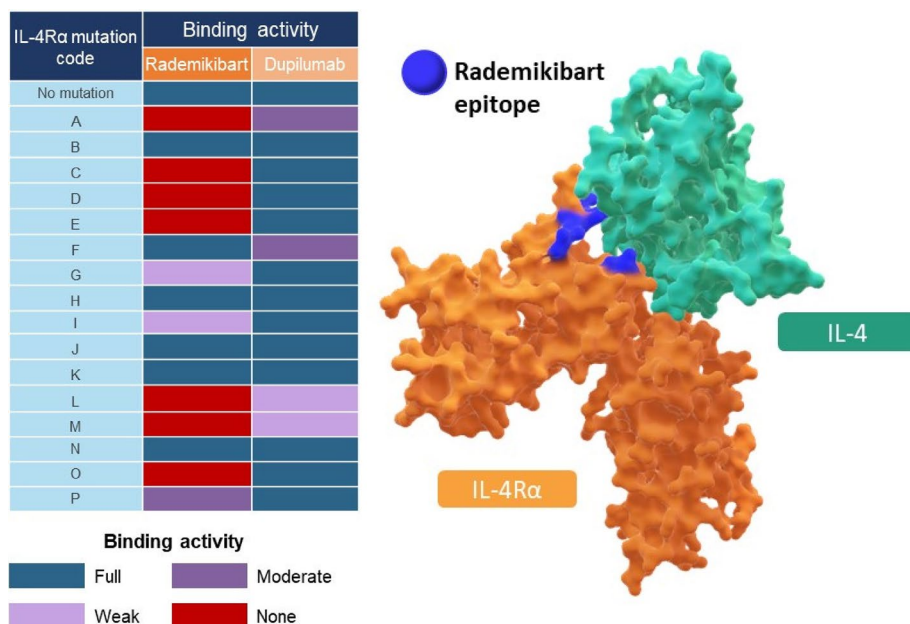
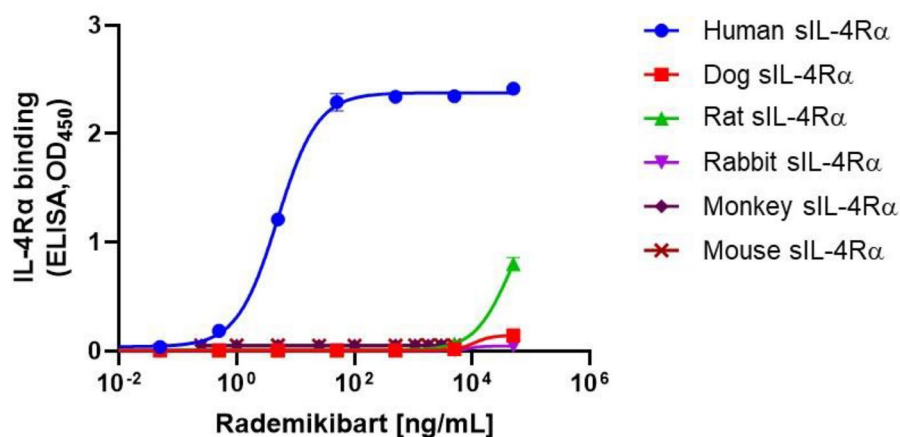


**Figure 1.** Rademikibart and dupilumab bind to distinct epitopes on human IL-4Rα. As shown in the table, mutation of amino acid residues (coded as A, C, D, E, L, M, and O), which are crucial for IL-4 binding, had little effect on the affinity for dupilumab but abolished binding of rademikibart, when assessed by ELISA. A more detailed version of the table (detailing the amino acid mutations associated with each mutation code letter and EC<sub>50</sub> values) is shown in Supplementary Fig. 1. Binding epitopes for rademikibart on human IL-4Rα are shown in the figure, based on the mutational analysis\*. EC<sub>50</sub> half maximal effective concentration. \*Mutation G is based on mutation of two amino acids; a stable single mutant could not be created, therefore both residues are highlighted blue in the figure.



	Human sIL-4Rα	Dog sIL-4Rα	Rat sIL-4Rα	Rabbit sIL-4Rα	Monkey sIL-4Rα	Mouse sIL-4Rα
IC <sub>50</sub> ng/mL)	4.9	N.D.	> 45058	N.D.	N.D.	N.D.

**Figure 2.** Rademikibart is specific for human IL-4Rα. Rademikibart bound to human sIL-4Rα with a K<sub>D</sub> of 106 pM and IC<sub>50</sub> of 4.9 ng/mL, but did not cross react with sIL-4Rα of other species (two or three replicates per species). IC<sub>50</sub> half maximal inhibitory concentration, K<sub>D</sub> equilibrium dissociation constant, N.D. not detected, sIL-4Rα soluble IL-4Rα.

Cytokine stimulation	Monoclonal antibody	IC <sub>50</sub> (ng/mL)					
		STAT6 signaling	p value	TF-1 cell proliferation	p value	TARC secretion	p value
IL-4	Rademikibart	7.0 ± 2.5	<0.01	8.0 ± 1.6	0.09	59.2 ± 3.9	0.11
	Dupilumab	9.9 ± 2.7		10.8 ± 1.1		65.2 ± 5.5	
IL-13	Rademikibart	6.6 ± 1.5	0.03	9.7 ± 0.8	0.20	13.5 ± 0.2	0.41
	Dupilumab	9.7 ± 2.5		12.0 ± 2.4		10.8 ± 2.7	

**Table 2.** Rademikibart inhibits cytokine-induced intracellular STAT6 signaling, TF-1 cell proliferation, and TARC secretion, generally with trends towards greater potency than dupilumab. Curve diagrams are shown in Supplementary Fig. 2. IC<sub>50</sub> expressed as mean ± standard deviation. *p* values for rademikibart versus dupilumab. Intracellular signaling was assessed using the HEK Blue™ STAT6 reporter cell assay. TF-1 cell proliferation was quantified using a cell counting kit-8. TARC secretion from PBMCs was quantified by ELISA. HEK human embryonic kidney, IC<sub>50</sub> half maximal inhibitory concentration, PBMC primary human peripheral blood mononuclear cells.

**Rademikibart inhibits ovalbumin-induced Th2 allergy in a mouse model.** Subcutaneous administration of rademikibart or dupilumab (25 mg/kg) to B-hIL-4/hIL-4RA mice during the OVA recall phase ameliorated several Th2-driven allergic responses (8 mice per treatment; Fig. 4A–F). Compared with the hIgG4 isotype control, both treatments almost completely eliminated the increased number of immune cells (CD45+ hematopoietic cells and eosinophils; *p* < 0.0001) and ovalbumin-specific IgE concentration in the blood (*p* < 0.01), as well as eosinophil infiltration in lung tissue (*p* < 0.0001). Airway mucus scores decreased by 60% with rademikibart treatment, reaching statistical significance versus the hIgG4 isotype control (*p* < 0.05), whereas the 50% reduction with dupilumab was not significant either versus the control or rademikibart (Fig. 4E). Based on medication-specific antibody concentrations in wildtype mice (3 mice per time point, per treatment [5 mg/kg]), a non-significant trend towards greater quantity of rademikibart than dupilumab was detected in bronchoalveolar lavage fluid (BALF) within 48 h post-treatment, despite similar blood exposure (Fig. 4G).

**Rademikibart downregulates expression of inflammatory genes in Th2-stimulated human skin.** Following Th2 stimulation, IL-4, IL-13, and TARC gene expression was upregulated in healthy human skin from two independent donors (Fig. 5). Rademikibart (10 µg/mL) downregulated the expression of all three genes in the Th2-stimulated explants. When compared head-to-head with dupilumab (10 µg/mL), the reduction in IL-4 expression was significantly greater with rademikibart, and there was a non-significant trend towards greater reduction in IL-13 with rademikibart (Fig. 5). For instance, in explants from Donor #1 (three or four explants analyzed per group), IL-4 gene expression was 12.3-fold higher following Th2 stimulation versus unstimulated tissue (*p* < 0.001), and decreased to 2.0-fold versus 8.2-fold higher with rademikibart versus dupilumab pretreatment, respectively (*p* < 0.01 comparing the two monoclonal antibodies), than in unstimulated tissue.

## Discussion

This is the first description of the immunological characterization of rademikibart, a next-generation monoclonal antibody targeting human IL-4Ra. We demonstrated that rademikibart bound with high affinity to human IL-4Ra, without cross-reaction to other mammalian IL-4Ra, resulting in potent downregulation of Th2-driven inflammation in vitro, in vivo (transgenic mice), and ex vivo (human skin). All experiments (except for cross-species IL-4Ra binding of rademikibart) were head-to-head with dupilumab, a currently marketed IL-4Ra targeting therapy for Th2-driven inflammatory diseases (AD, asthma, chronic rhinosinusitis with nasal polyposis, eosinophilic esophagitis, and prurigo nodularis)<sup>32,35–37,40,41</sup>. Notably, these head-to-head experiments indicated improved target engagement properties—based on the binding affinity of rademikibart (K<sub>D</sub> 20.7 pM) for human IL-4Ra, via an epitope distinct from dupilumab (K<sub>D</sub> 45.8 pM), for which some epitope mapping has previously been published<sup>42,43</sup>—and resulted in potent inhibition of Th2-driven inflammation that was at least comparable and potentially superior to dupilumab.

The improvements in Th2-driven inflammatory responses by rademikibart were demonstrated using a diverse collection of in vitro cellular systems. IL-4 and IL-13, when engaged with their cognate receptor, trigger intracellular activation of the Janus kinase (JAK)-signal transduction and activator of the STAT6 pathway<sup>44</sup>, and are growth factors for the TF-1 cell line<sup>45</sup>. Another molecule, TARC, recruits Th2 cells to inflammatory sites and is a clinical biomarker of AD activity<sup>30,31</sup>. All rademikibart-induced in vitro reductions in Th2-driven inflammation (IL-4 and IL-13-mediated JAK-STAT intracellular signaling, TF-1 cell proliferation, and TARC production) were concentration-dependent. Compared with dupilumab, rademikibart was more potent at inhibiting STAT6 signaling, with non-significant trends towards greater potency at reducing TF-1 cell proliferation, and similar potency when downregulating TARC production.

Given the highly selective binding of rademikibart to human IL-4Ra, and not to IL-4Ra from any other mammalian species, experiments were conducted with genetically modified mice; expression of mouse IL-4Ra and its IL-4 ligand was fully replaced by the human proteins. Beyond in vitro T cell-mediated Th2 responses, rademikibart resulted in concentration-dependent inhibition of IL-4 and IL-13-mediated activation of primary B cells, with a potency similar to dupilumab, in experiments with murine splenocytes. The in vivo ovalbumin-induced

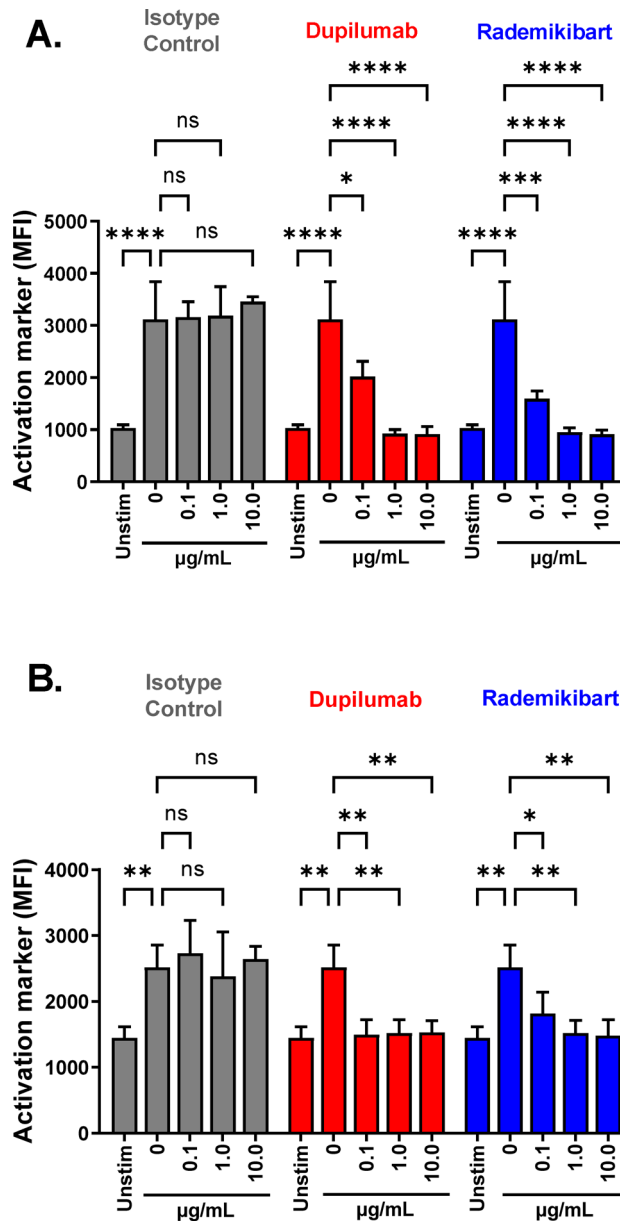


**Figure 3.** Rademikibart inhibits cytokine-induced B cell activation. Splenocytes were isolated from double humanized IL-4/IL-4RA (B-hIL4/hIL4RA) mice. Incubation with rademikibart resulted in concentration-dependent inhibition of (A) IL-4-induced CD23 and (B) IL-13-induced MHCII expression, analyzed by flow cytometry. ‘Unstim’ shows B cell activation marker expression without cytokine stimulation. The ‘0 µg/mL’ monoclonal antibody groups served as positive controls. No statistically significant differences in B cell activation marker expression were observed when comparing each concentration of rademikibart vs dupilumab.  $N = 3$  mice per group. Data are expressed as mean  $\pm$  standard deviation. One-way ANOVA and post hoc test ( $*p < 0.05$ ,  $**p < 0.01$ ,  $***p < 0.001$ ,  $****p < 0.0001$ , *ns* not significant).

Th2 allergy mouse model is well characterized and validated<sup>46,47</sup>. During the allergen (ovalbumin) recall inflammatory response, subcutaneous administration of rademikibart significantly ameliorated accumulation of CD45+ hematopoietic cells and eosinophils in the blood. Allergen-specific IgE blood titers were also significantly reduced, consistent with the in vitro B cell inhibition data. Similarly, blinded histological analysis of lung target tissue revealed significant reductions in the amount of airway mucus and eosinophil infiltration. Interestingly, despite similar blood exposure, there was a trend for rademikibart to distribute more rapidly into BALF than dupilumab in wildtype mice. Whether this tendency towards enhanced lung tissue exposure to rademikibart corresponded to the small difference in mucus score with rademikibart (60% decrease) versus dupilumab (50% decrease) in the mouse model remains unclear (the 60% reduction in mucus score with rademikibart reached statistical significance versus hIgG4 isotype control ( $p < 0.05$ ), whereas the 50% reduction with dupilumab was not significant versus both hIgG4 isotype control and rademikibart).

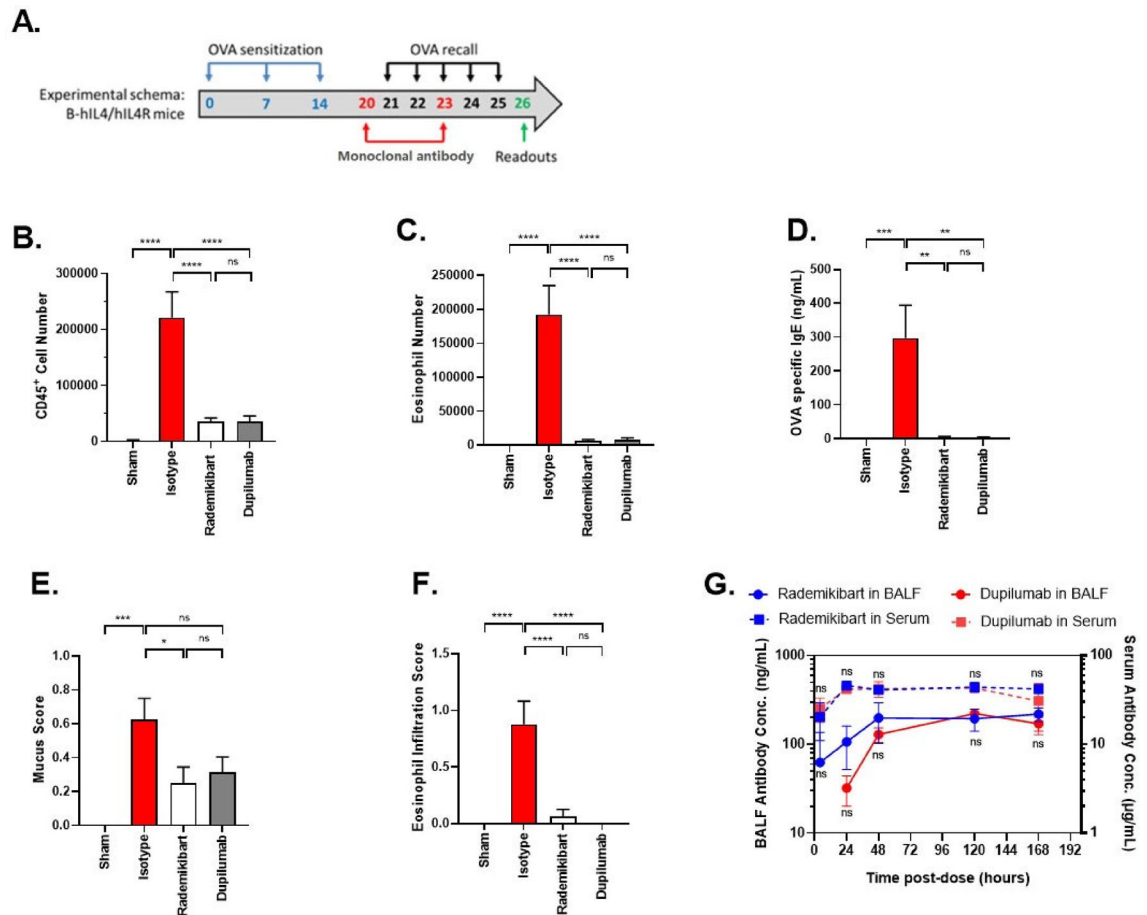


**Figure 4.** Rademikibart ameliorates Th2-driven allergic responses. (A) Schematic design of the ovalbumin-induced lung inflammation mouse model (time is shown in days), with humanized IL-4/IL-4RA (B-hIL4/hIL4RA) mice (N = 8 per group). In the mouse model, subcutaneous administration of rademikibart or dupilumab (25 mg/kg; on Days 20 and 23) resulted in reductions (on Day 26) in the total number of (B) CD45<sup>+</sup> hematopoietic cells and (C) eosinophils in alveolar lavage fluid, (D) ovalbumin-specific serum IgE concentration, (E) airway mucus score, and (F) eosinophil infiltration. (G) In wildtype mice (N = 3 per time point, per treatment), within 48 h post-treatment (5 mg/kg), there was a non-significant trend towards higher rademikibart-specific antibody concentrations than for dupilumab in bronchoalveolar lavage fluid (BALF), despite similar concentrations in serum (BALF antibody concentration for dupilumab at 4 h post-treatment was lower than the test limit). No statistically significant differences were observed with rademikibart vs dupilumab in the mouse model or in the wildtype mice. Data are expressed as mean  $\pm$  standard error of the mean. One-way ANOVA and post hoc test (\* $p$  < 0.05, \*\* $p$  < 0.01, \*\*\* $p$  < 0.001, \*\*\*\* $p$  < 0.0001, ns not significant).

Analyses of ex vivo Th2-stimulated human skin corroborated the in vitro and in vivo findings. Rademikibart rapidly downregulated IL-4, IL-13 and TARC expression in skin explants from two independent donors. Intriguingly, in these head-to-head ex vivo experiments, rademikibart was significantly more effective than dupilumab at inhibiting IL-4 gene expression, with a non-significant trend towards superiority for IL-13 gene expression, when both treatments were administered at the same concentration (10  $\mu$ g/mL). This finding may be related to greater soft tissue exposure with rademikibart than dupilumab, observed in the mouse model.

In summary, this manuscript represents the first immunological characterization of rademikibart, a highly potent and selective monoclonal antibody targeting human IL-4Ra. Reductions in inflammatory responses were observed in vitro (in intracellular STAT6 signaling, TF-1 cell proliferation, TARC release, and B cell activation), in vivo (in eosinophil infiltration and IgE release), and ex vivo (in IL-4, IL-13, and TARC gene expression). In these experiments, rademikibart was at least comparable, and potentially superior in vitro and ex vivo, to the currently approved treatment targeting human IL-4Ra. Rademikibart is currently being evaluated in Phase 2 clinical trials for the treatment of moderate-to-severe AD (NCT04444752, NCT05017480) and persistent asthma (NCT04773678).

## Materials and methods

For the experiments reported here, the source of the investigational treatment (rademikibart) was the same as in the Phase 2 clinical trials. Rademikibart was discovered by screening potential candidate molecules for T cell modulatory activity<sup>48</sup>. Head-to-head experiments of rademikibart were in comparison with commercially available dupilumab (Dupixent<sup>®</sup>) or an in-house dupilumab analog produced by transient transfection of HEK293

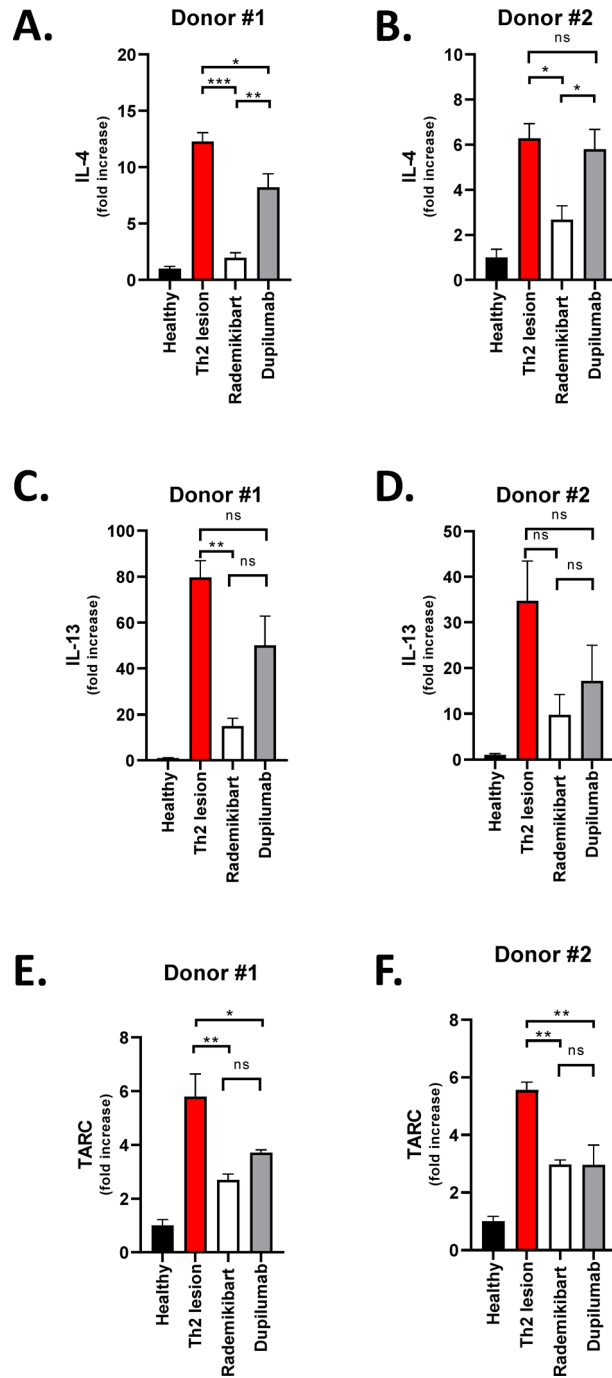


**Figure 5.** Rademikibart downregulates expression of inflammatory genes in Th2-stimulated human skin explants from two independent donors. Inflammatory genes investigated in Donors #1 and #2, respectively, were (A,B) IL-4, (C,D) IL-13, and (E,F) TARC. ‘Healthy’ shows gene expression without ex vivo Th2 stimulation or exposure to either monoclonal antibody. ‘Th2 lesion’ shows elevated gene expression in healthy skin explants exposed to a Th2 stimulation cocktail alone. ‘Rademikibart’ and ‘dupilumab’ show the effects of ex vivo pretreatment with each monoclonal antibody (10 µg/mL) on Th2-stimulated skin. Data are expressed as mean ± standard error of the mean. Three or four replicates per donor. One-way ANOVA and post hoc test (\* $p < 0.05$ , \*\* $p < 0.01$ , \*\*\* $p < 0.001$ , \*\*\*\* $p < 0.0001$ , ns not significant).

cells (Thermo Fisher Scientific, USA). Two vectors were used to produce the analog, pFUSE-CHIg-hG4 and pFUSE2-CLIg-hK (InvivoGen, USA). Dupilumab heavy and light chain V-region sequences were inserted into pFUSE-CHIg-hG4 and pFUSE2-CLIg-hK, respectively. HEK293 cells were transfected with the two vectors at a ratio of 1:1.

**Binding affinity to IL-4R $\alpha$ .** Two surface plasmon resonance protocols were used. *Protocol A:* Histidine tagged sIL-4R $\alpha$  was immobilized onto a treated CM5 sensor chip, to capture rademikibart or dupilumab analytes at different concentrations. *Protocol B:* Rademikibart or dupilumab were immobilized onto IgG Fc CM5 sensor chips, to capture sIL-4R $\alpha$  analyte at different concentrations. Data were acquired with the Biacore 8K (GE, USA) and equilibrium dissociation constant ( $K_D$ ), association rate constant ( $k_a$ ), and dissociation rate constant ( $k_d$ ) calculated.

**IL-4R $\alpha$  epitope mapping.** Site-specific mutations and alanine scanning mutations were incorporated into sIL-4R $\alpha$  to identify epitopes that bind to rademikibart or dupilumab antibodies. An in-house ELISA was used to evaluate the binding activity of rademikibart or dupilumab to the sIL-4R $\alpha$  mutants using a Flex Station 3 (Molecular Devices, USA) and half maximal effective concentration ( $EC_{50}$ ) calculated. See the Supplementary Methods section for information about the in-house ELISA.

**Cross-species IL-4R $\alpha$  binding.** Binding of rademikibart to human, cynomolgus monkey, dog, rat, rabbit, and mouse IL-4R $\alpha$  was evaluated using an in-house ELISA. Colorimetric change of TMB solution was detected using a Flex Station 3 and  $K_D$  calculated.

**Cytokine-induced intracellular signaling.** HEK Blue™ IL-4/IL-13 cells containing a STAT6 reporter gene (Invivogen, USA) were stimulated with 0.5 ng/mL IL-4 or 2.5 ng/mL IL-13, either alone or in the presence of rademikibart or dupilumab. As per the manufacturer's instructions, STAT6 activation was quantified via secreted alkaline phosphatase hydrolysis of QUANTI-Blue™ substrate colorimetric change. Data were acquired with the Flex Station 3 and half maximal inhibitory concentration ( $IC_{50}$ ) calculated.

**Binding to TF-1 cells and cytokine-induced TF-1 cell proliferation.** TF-1 human erythroid leukemia cells (ATCC, USA) were suspended in 45  $\mu$ L FACS buffer (PBS with 0.5% BSA). For the TF-1 cell binding experiments, rademikibart or dupilumab were added to the solution (100  $\mu$ g/mL) and, after incubating on ice for 30 min, the cells were washed twice and resuspended in 45  $\mu$ L FACS buffer. Following the addition of goat anti-human IgG(H+L) Alexa Fluor 488 (Invitrogen, China), another 30-min incubation on ice and two more cell washes, rademikibart and dupilumab binding was detected by flow cytometry (BD Calibur).

For the TF-1 cell proliferation experiments, the cells were stimulated with IL-4 (0.5 ng/mL) or IL-13 (5 ng/mL; Sino Biological, China), followed by the addition of rademikibart or dupilumab. TF-1 cell proliferation was quantified after 72 h using a cell counting kit-8 (CCK-8, Beyotime, China) as per the manufacturer's instructions. Data were acquired with the Flex Station 3 and  $IC_{50}$  calculated.

**Cytokine-induced TARC release.** PBMCs (Sailybio, China) were stimulated with IL-4 (2 ng/mL) or IL-13 (1 ng/mL). Rademikibart or dupilumab were added to the culture for 72 h and supernatants collected. Human TARC concentrations were quantified by ELISA (Abcam, UK) as per the manufacturer's instructions. Data were acquired with the Flex Station 3 and  $IC_{50}$  calculated.

**Cytokine-induced B cell activation.** B-hIL4/hIL4RA mice (Biocytogen, China) express human IL-4 and IL-4RA, replacing their murine counterparts<sup>47</sup>. Splenocytes were isolated from B-hIL4/hIL4RA mice and incubated with human IgG4 isotype control (CrownBio, USA), rademikibart or dupilumab (0.1, 1.0, or 10.0  $\mu$ g/mL), in the presence of human IL-4 (50 pM) or IL-13 (50 nM) (Preprotech, USA). After 72 h, B cell activation was analyzed by flow cytometry, using CD23 or MHCII as activation markers (Biolegend, USA). Data were acquired with NxT software (Invitrogen, USA) and mean fluorescence intensity was analyzed.

**Ovalbumin-induced Th2 allergy mouse model.** The ovalbumin-induced Th2 allergy mouse model is well characterized and validated<sup>46,47</sup>. B-hIL-4/hIL-4RA mice (Biocytogen, China) were sensitized with 200  $\mu$ L intraperitoneal injections of 200 mg/mL ovalbumin (Sigma, USA) in PBS on Days 0, 7, and 14. Rademikibart or dupilumab (25 mg/kg) was subcutaneously administered on Days 20 and 23. On Days 21–25, mice inhaled atomized 2% ovalbumin for 30 min each day, triggering a Th2-driven recall response.

At termination, alveolar lavage fluid was collected, stained for CD45+ hematopoietic cells and eosinophils, and analyzed by flow cytometry. Markers comprised of mouse CD45 (Biolegend, USA), Siglec-F (BD Biosciences, USA), CD11c (eBioscience, USA), Ly6G (Biolegend), CD11b (BD Horizon, USA), CD16 (eBioscience, USA).

Serum samples were analyzed for ovalbumin-specific IgE via ELISA (Chondrex, USA).

Lung tissues (without lavage) were formalin fixed, paraffin embedded, sectioned (7  $\mu$ m), and stained with hematoxylin and eosin. Histological changes (inflammatory cell infiltration around the blood vessels and bronchi, mucus in the bronchi and trachea, eosinophil infiltration around the blood vessels and bronchi) were scored by a pathologist unaware of the treatment groups. Scores were assigned in 0.5 increments ranging from 0 (no visual lesion) through to 1.5 (approximately 20% of the total area was affected).

**Exposure to rademikibart and dupilumab in wildtype mice.** Exposure to rademikibart and dupilumab (5 mg/kg) in serum and BALF was determined at 4, 24, 48, 120, and 168 h post-treatment, based on medication-specific antibody concentrations in CD-1 wildtype mice (Beijing Vital River Laboratory Animal Technology, China). An in-house ELISA was used to evaluate the binding activity of rademikibart or dupilumab to sIL-4R $\alpha$  using a Flex Station 3.

**Ex vivo human skin.** Ex vivo human skin (ca. 750  $\mu\text{m}$  thickness), from two independent adult donors without dermatological conditions, was sectioned using a 7 mm punch biopsy and placed into a Transwell insert, as previously as described<sup>49</sup>. Rademikibart or dupilumab were applied in cornification media (10  $\mu\text{g}/\text{mL}$ ). After overnight pretreatment, the media was vacuum-aspirated and fresh media was added containing stimulation cocktail (Th2; MedPharm, UK) and fresh therapeutic compound. The skin explants were harvested 24 h after commencement of stimulation, placed in RNAlater solution, and stored at 5 °C. RNA was isolated using the Kingfisher robotic RNA prep system (ThermoFisher, USA) and normalized prior to cDNA synthesis using the High Capacity cDNA Reverse Transcription Kit (Applied Biosystems, USA). Synthesized cDNA samples were diluted in RNase-free water, transferred to an optical 384-well plate (in duplicate), and TaqMan™ Gene Expression Master Mix (Applied Biosystems, USA) was added for RT-qPCR analysis of inflammation biomarkers.

qPCR values were calculated using the relative quantification approach. The Ct value (threshold cycle) is defined as the fractional cycle number at which the amount of amplified target reaches a fixed threshold. As qPCR run on a log<sub>2</sub> scale, logarithmic calculations are used. Ct values were determined for target genes and a single normalizer gene (GAPDH) for each sample. To determine the  $\Delta$  Ct for each sample, the Ct for the normalizer gene was subtracted from the Ct for the target gene. Data was normalized to the unstimulated skin sample.

**Study ethics and conduct.** Research reported herein received ethics committee approval (Institutional Animal Care and Use Committee, Biocytogen, and MedPharm) prior to commencement and was performed by Connect Biopharma and MedPharm in accordance with relevant institutional and national guidelines and regulations.

Experiments with ex vivo human tissue were conducted in accordance with the Declaration of Helsinki; skin explants were obtained after the participants provided informed written consent, including for publication of the results. Reporting of animal experiments was in accordance with ARRIVE guidelines.

Animal studies were performed in Association for Assessment and Accreditation of Laboratory Animal Care (AAALAC)-accredited facilities. All animals were housed under specific pathogen-free conditions in individual ventilated cages and reared in line with standardized methods (20–26 °C, 40–70% humidity, 12-hour light/dark cycle, free access to food and water).

**Statistical analysis.** Calculations ( $K_D$ ,  $k_a$ ,  $k_d$ ,  $IC_{50}$ , and  $EC_{50}$ ) and statistical analysis were performed using GraphPad Prism (GraphPad Software Inc, USA). Differences between groups were assessed by one-way ANOVA with Tukey's multiple comparisons test. Statistical significance was defined by  $p < 0.05$ .

### Data availability

The raw data supporting the conclusions of this article will be made available by the authors, without undue reservation (corresponding author: Xin Yang, DSc, xyang@connectpharm.com).

Received: 14 March 2023; Accepted: 23 July 2023

Published online: 31 July 2023

### References

- To, T. *et al.* Global asthma prevalence in adults: Findings from the cross-sectional world health survey. *BMC Public Health* **12**, 204 (2012).
- Enilari, O. & Sinha, S. The global impact of asthma in adult populations. *Ann. Glob. Health* **85**, 2 (2019).
- Lai, C. K. W. *et al.* Global variation in the prevalence and severity of asthma symptoms: Phase three of the International Study of Asthma and Allergies in Childhood (ISAAC). *Thorax* **64**, 476–483 (2009).
- Janson, C. *et al.* The European Community Respiratory Health Survey: What are the main results so far?. *Eur. Respir. J.* **18**, 598–611 (2001).
- Asher, M. I., García-Marcos, L., Pearce, N. E. & Strachan, D. P. Trends in worldwide asthma prevalence. *Eur. Respir. J.* **56**, 2002094 (2020).
- Eichenfield, L. F. *et al.* Guidelines of care for the management of atopic dermatitis. *J. Am. Acad. Dermatol.* **70**, 338–351 (2014).
- Chovatiya, R. & Silverberg, A. I. Pathophysiology of atopic dermatitis and psoriasis: Implications for management in children. *Children* **6**, 108 (2019).
- Mathiesen, S. M. & Thomsen, S. F. The prevalence of atopic dermatitis in adults: Systematic review on population studies. *Dermatol. Online J.* **25**, 13030 (2019).
- Garg, N. & Silverberg, J. I. Epidemiology of childhood atopic dermatitis. *Clin. Dermatol.* **33**, 281–288 (2015).
- Boguniewicz, M. *et al.* Expert perspectives on management of moderate-to-severe atopic dermatitis: A multidisciplinary consensus addressing current and emerging therapies. *J. Allergy Clin. Immunol. In Pract.* **5**, 1519–1531 (2017).
- Chiesa Fuxench, Z. C. *et al.* Atopic dermatitis in America study: A cross-sectional study examining the prevalence and disease burden of atopic dermatitis in the US adult population. *J. Investig. Dermatol.* **139**, 583–590 (2019).
- Akinbami, L. J., Moorman, J. E. & Liu, X. Asthma prevalence, health care use, and mortality: United States, 2005–2009. *Natl Health Stat Report* 1–14 (2011).
- Centers for Disease Control and Prevention. 2020 National Health Interview Survey (NHIS) Data. <https://www.cdc.gov/asthma/nhis/2020/table4-1.htm>
- Silverberg, J. I., Garg, N. K., Paller, A. S., Fishbein, A. B. & Zee, P. C. Sleep disturbances in adults with eczema are associated with impaired overall health: A US population-based study. *J. Investig. Dermatol.* **135**, 56–66 (2015).
- Roche, N. *et al.* Real-life impact of uncontrolled severe asthma on mortality and healthcare use in adolescents and adults: Findings from the retrospective, observational RESONANCE study in France. *BMJ Open* **12**, e060160 (2022).
- Patel, N. U., D'Ambra, V. & Feldman, S. R. Increasing adherence with topical agents for atopic dermatitis. *Am. J. Clin. Dermatol.* **18**, 323–332 (2017).
- Simpson, E. L. *et al.* When does atopic dermatitis warrant systemic therapy? Recommendations from an expert panel of the International Eczema Council. *J. Am. Acad. Dermatol.* **77**, 623–633 (2017).
- Matsumoto-Sasaki, M. *et al.* Association of longitudinal changes in quality of life with comorbidities and exacerbations in patients with severe asthma. *Allergol. Int.* **71**, 481–489 (2022).

19. Dalgard, F. J. *et al.* The psychological burden of skin diseases: A cross-sectional multicenter study among dermatological out-patients in 13 European countries. *J. Investig. Dermatol.* **135**, 984–991 (2015).
20. Schonmann, Y. *et al.* Atopic eczema in adulthood and risk of depression and anxiety: A population-based cohort study. *J. Allergy Clin. Immunol. In Pract.* **8**, 248–257.e16 (2020).
21. Silverberg, J. I. *et al.* Symptoms and diagnosis of anxiety and depression in atopic dermatitis in U.S. adults. *Br. J. Dermatol.* **181**, 554–565 (2019).
22. Xie, Q.-W., Dai, X., Tang, X., Chan, C. H. Y. & Chan, C. L. W. Risk of mental disorders in children and adolescents with atopic dermatitis: A systematic review and meta-analysis. *Front. Psychol.* **10**, 1773 (2019).
23. Fleischmann, R. Recent issues in JAK inhibitor safety: Perspective for the clinician. *Expert Rev. Clin. Immunol.* **18**, 295–307 (2022).
24. Pelaia, C. *et al.* Interleukins 4 and 13 in Asthma: Key pathophysiologic cytokines and druggable molecular targets. *Front. Pharmacol.* **13**, 851940 (2022).
25. Chan, S. C. *et al.* Abnormal IL-4 gene expression by atopic dermatitis T lymphocytes is reflected in altered nuclear protein interactions with IL-4 transcriptional regulatory element. *J. Investig. Dermatol.* **106**, 1131–1136 (1996).
26. Yang, X., Kambe, N., Takimoto-Ito, R. & Kabashima, K. Advances in the pathophysiology of atopic dermatitis revealed by novel therapeutics and clinical trials. *Pharmacol. Ther.* **224**, 107830 (2021).
27. Neis, M. *et al.* Enhanced expression levels of IL-31 correlate with IL-4 and IL-13 in atopic and allergic contact dermatitis. *J. Allergy Clin. Immunol.* **118**, 930–937 (2006).
28. Saha, S. K. *et al.* Increased sputum and bronchial biopsy IL-13 expression in severe asthma. *J. Allergy Clin. Immunol.* **121**, 685–691 (2008).
29. Antczak, A. *et al.* Analysis of changes in expression of IL-4/IL-13/STAT6 pathway and correlation with the selected clinical parameters in patients with atopic asthma. *Int. J. Immunopathol. Pharmacol.* **29**, 195–204 (2016).
30. Renert-Yuval, Y. *et al.* Biomarkers in atopic dermatitis—A review on behalf of the International Eczema Council. *J. Allergy Clin. Immunol.* **147**, 1174–1190.e1 (2021).
31. Kataoka, Y. Thymus and activation-regulated chemokine as a clinical biomarker in atopic dermatitis. *J. Dermatol.* **41**, 221–229 (2014).
32. Simpson, E. L. *et al.* Two phase 3 trials of dupilumab versus placebo in atopic dermatitis. *N. Engl. J. Med.* **375**, 2335–2348 (2016).
33. Guttman-Yassky, E. *et al.* Efficacy and safety of lebrikizumab, a high-affinity interleukin 13 inhibitor, in adults with moderate to severe atopic dermatitis: A phase 2b randomized clinical trial. *JAMA Dermatol.* **156**, 411 (2020).
34. Blauvelt, A. *et al.* Tralokinumab efficacy and safety, with or without topical corticosteroids, in North American adults with moderate-to-severe atopic dermatitis: A subanalysis of phase 3 trials ECZTRA 1, 2, and 3. *Dermatol. Ther. (Heidelb.)* <https://doi.org/10.1007/s13555-022-00805-y> (2022).
35. Busse, W. W. *et al.* Liberty asthma QUEST: Phase 3 randomized, double-blind, placebo-controlled, parallel-group study to evaluate dupilumab efficacy/safety in patients with uncontrolled, moderate-to-severe asthma. *Adv. Ther.* **35**, 737–748 (2018).
36. Mullol, J. *et al.* Efficacy and safety of dupilumab in patients with uncontrolled severe chronic rhinosinusitis with nasal polyps and a clinical diagnosis of NSAID-ERD: Results from two randomized placebo-controlled phase 3 trials. *Allergy* **77**, 1231–1244 (2022).
37. Hirano, I. *et al.* Efficacy of dupilumab in a phase 2 randomized trial of adults with active eosinophilic esophagitis. *Gastroenterology* **158**, 111–122.e10 (2020).
38. Pelaia, C. *et al.* Real-life effects of dupilumab in patients with severe type 2 asthma, according to atopic trait and presence of chronic rhinosinusitis with nasal polyps. *Front. Immunol.* **14**, 1121237 (2023).
39. Mimmi, S. *et al.* Spotlight on a short-time treatment with the IL-4/IL-13 receptor blocker in patients with CRSwNP: MicroRNAs modulations and preliminary clinical evidence. *Genes* **13**, 2366 (2022).
40. Yosipovitch, G. *et al.* Dupilumab in patients with prurigo nodularis: Two randomized, double-blind, placebo-controlled phase 3 trials. *Nat. Med.* <https://doi.org/10.1038/s41591-023-02320-9> (2023).
41. Dupilumab FDA label. [https://www.accessdata.fda.gov/drugsatfda\\_docs/label/2022/761055s046lbl.pdf](https://www.accessdata.fda.gov/drugsatfda_docs/label/2022/761055s046lbl.pdf)
42. Tahir, S. *et al.* Accurate determination of epitope for antibodies with unknown 3D structures. *MAbs* **13**, 1961349 (2021).
43. Kim, J.-E. *et al.* Engineering of anti-human interleukin-4 receptor alpha antibodies with potent antagonistic activity. *Sci. Rep.* **9**, 7772 (2019).
44. Geha, R. S., Jabara, H. H. & Brodeur, S. R. The regulation of immunoglobulin E class-switch recombination. *Nat. Rev. Immunol.* **3**, 721–732 (2003).
45. Lefort, S., Vita, N., Reeb, R., Caput, D. & Ferrara, P. IL-13 and IL-4 share signal transduction elements as well as receptor components in TF-1 cells. *FEBS Lett.* **366**, 122–126 (1995).
46. Ashino, S. *et al.* Janus kinase 1/3 signaling pathways are key initiators of TH2 differentiation and lung allergic responses. *J. Allergy Clin. Immunol.* **133**, 1162–1174.e4 (2014).
47. Yan, P. *et al.* The establishment of humanized IL-4/IL-4RA mouse model by gene editing and efficacy evaluation. *Immunobiology* **225**, 151998 (2020).
48. Connect Biopharma. Our Science. <https://www.connectbiopharm.com/our-science/>
49. Neil, J. E., Brown, M. B. & Williams, A. C. Human skin explant model for the investigation of topical therapeutics. *Sci. Rep.* **10**, 21192 (2020).

## Acknowledgements

Writing support was provided by Michael Jonathan Riley, PhD, Fortis Pharma Consulting, with financial support by Connect Biopharma LLC (San Diego, USA). We would like to thank Raúl Collazo (Connect Biopharma LLC (San Diego, USA) for reviewing the manuscript.

## Author contributions

P.S., X.Y., L.Z., Y.D., and Q.W. contributed equally to performing the experiments. W.P. and Z.W. were involved in experimental planning and data interpretation. P.S. prepared the manuscript. All authors reviewed and approved the manuscript.

## Funding

This study was funded by Connect Biopharma LLC (San Diego, USA).

## Competing interests

All authors are current or former employees or shareholders of Connect Biopharma LLC.

### Additional information

**Supplementary Information** The online version contains supplementary material available at <https://doi.org/10.1038/s41598-023-39311-2>.

**Correspondence** and requests for materials should be addressed to X.Y.

**Reprints and permissions information** is available at [www.nature.com/reprints](http://www.nature.com/reprints).

**Publisher's note** Springer Nature remains neutral with regard to jurisdictional claims in published maps and institutional affiliations.



**Open Access** This article is licensed under a Creative Commons Attribution 4.0 International License, which permits use, sharing, adaptation, distribution and reproduction in any medium or format, as long as you give appropriate credit to the original author(s) and the source, provide a link to the Creative Commons licence, and indicate if changes were made. The images or other third party material in this article are included in the article's Creative Commons licence, unless indicated otherwise in a credit line to the material. If material is not included in the article's Creative Commons licence and your intended use is not permitted by statutory regulation or exceeds the permitted use, you will need to obtain permission directly from the copyright holder. To view a copy of this licence, visit <http://creativecommons.org/licenses/by/4.0/>.

© The Author(s) 2023